KSCE Journal of Civil Engineering (2021) 25(9):3376-3389
DOI 10.1007/s12205-021-0768-4

pISSN 1226-7988, eISSN 1976-3808
www.springer.com/12205

Structural Engineering

Corrosion Cracking Process of Reinforced Concrete under the Coupled Effects of Chloride and Fatigue Loading

Jiansheng Shen[a,b], **Junzhe Liu**[a], **Yidong Xu**[b,d], **Kanghao Jia**[b], **Fangyu Wu**[c], **Wei Chen**[b], **and Dayong Zhu**[b,d]

[a]*School of Civil Engineering and Environment, Ningbo University, Ningbo 315211, China*
[b]*School of Civil Engineering and Architecture, NingboTech University, Ningbo 315100, China*
[c]*School of Architecture and Engineering, Zhejiang University, Hangzhou 310058, China*
[d]*Ningbo Research Institute, Zhejiang University, Ningbo 315100, China*

ARTICLE HISTORY

Received 9 May 2020
Revised 13 November 2020
Accepted 14 April 2021
Published Online 1 July 2021

KEYWORDS

Coupled effect
Corrosion products
Model of steel rust cracking
Corrosion cracking process
Microscopic characteristics

ABSTRACT

To study the corrosion cracking process of reinforced concrete under the combined effects of chloride and fatigue loading, the constan-current and dry-wet cycle accelerated corrosion method was used to corrosion the specimens under different stress levels for different time. The quality loss of reinforcement, the composition of corrosion products and the cracking of concrete are analyzed from the macro, micro and micro scales, and to obtain the spatial distribution as well as microscopic characteristics of corrosion products of the reinforcement bar under coupling conditions. Additionally, a model of steel rust cracking under the coupled action of chloride and fatigue loading is established. The results show that: under the same corrosion time, the concrete cracking and steel corrosion degree become more serious with the increase of stress level. The greater the stress level, the earlier corrosion occurs and the more corrosion products are, Moreover, due to the fatigue load, the concrete on the upper side of the steel bar has rust expansion cracks earlier than the lower side.

1. Introduction

At present, reinforced concrete (RC) bridges are widely used in transportation. Due to the reciprocating effect of transportation, bridges are prone to fatigue (Nie et al., 2011; Shah et al., 2014; Liu et al., 2020). In addition, in coastal areas, chloride-induced erosion causes the deterioration of RC structures (Liu et al., 2018), such as steel corrosion, peeling of concrete covers and reduction in structural capacities (Vu and Steward, 2000). Corrosion-induced cracking is the major cause of durability deterioration in RC structures (Hartt, 2012). As steel corrosion develops, the corrosion product, which is approximately two to six times the volume of the original steel (Marcotte and Hansson, 2007), produces an expansive pressure on the surrounding concrete that leads to concrete-cover cracking. The cracks provide paths for the rapid ingress of aggressive agents into the reinforcement and accelerate the corrosion process (Asami and Kikuchi, 2003; Duffo et al., 2004), which reduces the load-bearing capacity and ductility of the structure (Yu et al., 2015) and results in progressive deterioration and even spalling of the concrete cover (Williamson and Clark, 2000). Therefore, investigation of corrosion-induced cracking is important for the prediction of the durability of reinforced concrete structures.

For RC structures in coastal regions, the service conditions consist of fatigue loading and chloride corrosion (Wu et al., 2018). According to the studies of Ahn and Reddy (2001) and Ren et al. (2015), steel corrosion in RC structures is usually more aggressive under cyclic loading (fatigue loading) than static loading.

A large number of studies have investigated the load-carrying capacity (Rodriguez et al., 1997), residual flexural capacity (Torres-Acosta et al., 2007), flexural stiffness (Dekoster et al., 2003) and load–deflection curves (Zhu and François, 2014) of corroded RC beams, taking into account the effects of stirrup corrosion (Vu et al., 2014), different types of reinforcing bars (Wang et al., 2015), size of tensile reinforcement (Azad et al., 2010) and bond strength degradation (Adelaide et al., 2012). The flexural behaviour of RC beams corroded under constant sustained service loads has been analysed (Malumbela et al., 2009). In addition to static

CORRESPONDENCE Junzhe Liu ljz_junzhe@163.com School of Civil Engineering and Environment, Ningbo University, Ningbo 315211, China

behaviour, the fatigue performance of RC beams has caused wide concern. The fatigue life (Pimentel et al., 2008), flexural stiffness (Higgins et al., 2013), crack width (Oh and Kim, 2007) and crack growth (Ray and Kishen, 2014) of RC beams under repeated loading have been investigated by various researchers. The nonlinear behaviour of cracked RC beams under variable stress amplitudes has been numerically simulated (Sousa et al., 2014). All of the investigations mentioned above examine the behaviour of RC beams under the influence of pure corrosion or pure fatigue. There has historically been little concern about the combined effects of corrosion and fatigue (Coca et al., 2011). Fang et al. (2013) experimentally investigated the flexural behaviour of corroded RC beams under repeated loading regarding the corrosion influence on bond strength as the most important factor and indicated that a low corrosion level increased the bond strength between concrete and reinforcing bar. Dong et al. (2017) investigated the cracking behaviour and flexural capacity of beams under simultaneous sus-tained loading and steel corrosion, and the results show that simultaneous loading and corrosion lead to more severe and faster cracking damage on the beams. Xu et al. (2018) described the coupled effects of chloride ingress and static loading on the evolution of corrosion of steel reinforcement in concrete, and found that the coupled action of chloride ingress and static loading, increased the non-uniform distribution of corrosion activity on the steel reinforcement significantly. Oyado et al. (2003) conducted fatigue loading tests of corroded RC beams and found that the reduction in fatigue strength was proportional to the weight loss of the reinforcing bar. Bastidas-Arteaga (2018) proposed a deterioration model for the application of fatigue loading to steel bars corroded by chloride ions and found that the total lifetime of RC structures was reduced by approximately 7%. Yi et al. (2010) investigated the performance of RC beams with corroded steel bars under fatigue loading and found that the fatigue life of RC beams decreased with increasing the degree of corrosion of the steel bar. Wu et al. (2020) investigated the effects of reinforcement ratio, and combined actions of initial fatigue damage and chloride corrosion on the fatigue behavior of beams, and found that the experimental method led to the pitting corrosion of tensile steels and hence considerably reduced the total fatigue life of RC beams. Mao et al. (2018) investigated the fatigue flexural performance of RC beams attacked by salt spray, and found that the experimental method can couple corrosion deterioration and fatigue loading reasonably. Lu et al. (2018) investigated experimentally the behavior of RC beams under simultaneous fatigue loading and steel corrosion, the results indicated that general and local corrosion occurred simultaneously under the joint effects of fatigue loading and corrosion, and it was also found that the flexural stiffness of RC beams increased in early loading cycles.

Wang et al. (2018a) investigated RC beams subjected to fatigue loading before 388 d of NaCl solution wet-dry cycles. The results confirmed the significant effect of initial loading damage on the lifetime assessment, especially in a corrosive environment. Sheng et al. (2017) investigated RC beams subjected to initial fatigue loading, followed by chloride corrosion and then fatigue ife testls. The results showed that after 6 months of NaCl solution wet-dry cycles, the crack width in initial fatigue-damaged RC beams increased. During the fatigue life tests that followed, the degradation of RC beams was accelerated with increasing deflection and decreasing stiffness. Sun et al. (2015) subjected RC beams to repeated fatigue loading after accelerated corrosion and studied the failure mode and flexural stiffness of corroded RC beams under repeated loading as well as the mechanical behaviour of reinforcing bars after corrosion fatigue. The results indicate that the flexural stiffness change in corroded RC beams under repeated loading has two obvious stages: a slowly decreasing stage and a stable stage.

Recently, the influence of fatigue loading on specimens has been gradually considered in research on the corrosion cracking of reinforced concrete, but most studies have separated the fatigue loading from the corrosion environment. In engineering practice, most of the specimens are in an environment where fatigue and corrosion are coupled. At present, concrete fatigue research mainly focuses on the concrete fatigue loading capacity, stiffness of concrete and concrete damage research. However, there are few studies on the micro-characteristics of reinforcement/concrete corrosion products, especially on the microanalysis of the transition layer and corrosion products of reinforced concrete under the coupled action of chloride and fatigue loading.

In this paper, reinforced concrete specimens were studied under the coupled effects of chloride and fatigue loading. Reinforced concrete specimens were subjected to the coupled effects of chloride and fatigue loading by using a fatigue loading device and constant-current dry-wet cycle accelerated corrosion device. After corrosion for a predetermined time, the corrosion of the reinforcement was studied with regards to the macroscopic, fine and microscopic scales, and the corrosion products were studied at the microscopic level. The corrosion cracking process of reinforced concrete under chloride-fatigue loading was studied.

2. Experiment

2.1 Materials

The dimensions of the reinforced concrete specimen used in the test were 150 mm × 150 mm × 550 mm, and the concrete cover thickness was 20 mm. Two HPB300 (hot-rolled plain steel bar, the grade of 300 MPa) reinforcement bars were used for longitudinal reinforcement (the measured mass was accurate to 0.001 g); the diameter was 10 mm, and the length was 500 mm. The mixing proportion of C35 concrete was cement:water:sand: coarse aggregate = 1:0.53:2:3. The cement was PO42.5 ordinary Portland cement. The water used was tap water; the fine aggregate was medium coarse sand, and the coarse aggregate was gravel with a particle size of 5 – 15 mm. The 28 d standard cube compressive strength of the concrete was measured, and the standard value of the average compressive strength of the concrete cube was 40.5 MPa. The reinforcement bars were placed into the concrete test block mould and placed on the 20 mm high concrete

Fig. 1. Schematic Diagram of the RC Specimen (mm)

pad block. The position of the reinforcement bars was adjusted so that the distance between the two bars and the mould wall on both sides was 25 mm. A schematic of the specimen is shown in Fig. 1.

2.2 Specimen Preparation

The specimen was made with reference to the"Standard for methods of long-term performance and durability of ordinary concrete" (GB/T 50082-2009, 2009). The reinforcement was cut off according to the design length. The reinforcement bars were pickled with 12% hydrochloric acid solution, and the rust was washed from the surface of the reinforcement bars. Then, the reinforcement bars were rinsed with water, and the washed reinforcement bars were put into lime water for neutralisation. Then, the reinforcement bars were rinsed with water, dried and placed into a drying oven to dry for 4 h. After the surface was wiped clean, each reinforcement bar was weighed by an electronic balance (accurate to 0.001 g) and labelled (1, 2, and 3). The two reinforcement bars in the specimen were connected with red and blue wires and sealed by insulating tape to facilitate the subsequent electrification and accelerate the corrosion (as shown in Fig. 2). The wires were drawn out of the mould, and the concrete was poured into the mould (as shown in Fig. 3).

2.3 Test Method

2.3.1 Accelerated Corrosion Method

Due to the advantages of the electric-accelerated corrosion method, such as its simplicity, high controllability, short time and low cost, this method has become the most commonly used method for corroding reinforced concrete specimens. Artificially accelerated

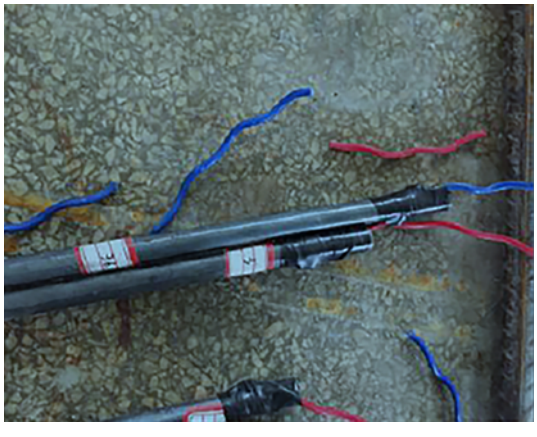

Fig. 2. Reinforcement Fabrication

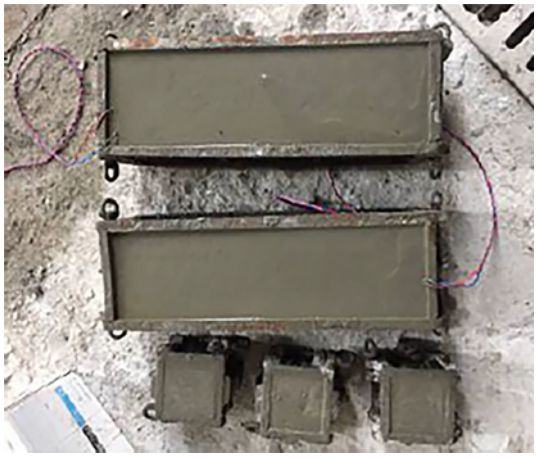

Fig. 3. Concrete Pouring

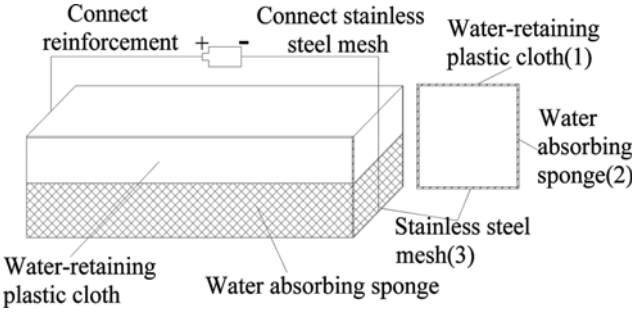

Fig. 4. Constant-Current Dry-Wet Cycle Accelerated Corrosion Device

corrosion is slightly different from that under natural conditions. Currently, scholars have proposed many accelerated corrosion methods that have non-uniform corrosion characteristics similar to those under natural conditions, among which the constant-current dry-wet cycle accelerated corrosion method proposed by Professor Jin Weiliang is a typical representative (Jin and Zhao, 2014). Based on the constant-current dry-wet cycle accelerated corrosion method by Jin, We made some changes in the experimental (as shown in Fig. 4), this method can not only accelerate the corrosion, but also better simulate the non-uniform corrosion of reinforcement (Xia et al., 2011; Dong et al., 2017; Mao et al., 2018; Xu et al., 2018; Zhang et al., 2020). Using this method, the corrosion morphology of reinforcement obtained by Xu and Dong is shown in Fig. 5.

1) A water-retaining plastic cloth, 2) water absorbing sponge and 3) stainless steel mesh were placed on the bottom of the specimen in sequence. The concrete specimen was wrapped with 3 layers of water-retaining plastic to prevent leakage during fatigue loading. The absorbent sponge was used to absorb sodium chloride solution to immerse the specimen in the solution. The concrete internal reinforcement and stainless steel mesh were connected with the positive and negative poles of the DC power supply to form a closed loop, making it an "electrolytic cell" to simulate the real non-uniform corrosion expansion of the reinforcement. A current density of 1.5 mA/cm^2 was applied during the accelerated corrosion process by using a DC power source.

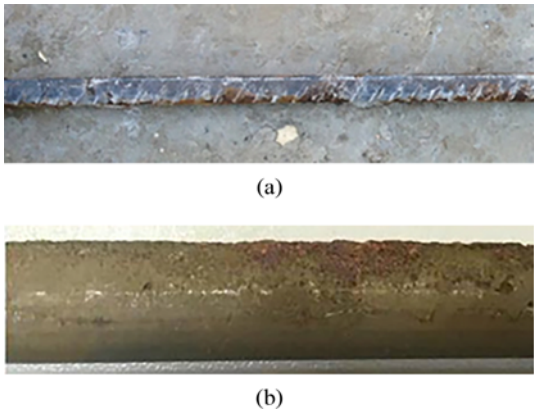

(a) (b)

Fig. 5. Non-uniform Corrosion of Reinforcement: (a) Dong et al., 2017, (b) Xu et al., 2018

2.3.2 Fatigue Loading Method

The wrapped specimen was placed on a 25 t fatigue test machine; a rolling bearing and a fixed bearing were placed 25 mm away from the two edges of the specimen; and fatigue loading was applied with the concentrated stress method, as shown in Fig. 6. Sinusoidal fatigue loading was applied with a loading frequency of 2.0 Hz, a stress ratio of 0.2, and stress levels of 0.3, 0.4 and 0.5. During the loading process, The corre-sponding upper limit value of fatigue stress for the tensile reinforcement was 78.8 MPa, 105.1 MPa and 131.3 MPa, respectively, and the lower limit value of fatigue stress was 15.7 MPa, 21.0 MPa, 26.2 MPa. At each stress level, the loading was applied for 36h, 72 h, 144 h and 216 h.

After the loading device was installed, the prepared 5% NaCl solution (Lu et al., 2016; Lu et al., 2018; Wang et al., 2018b) was poured into the water-retaining plastic cloth, and the sponge fully absorbed the solution and contacted the specimen for 24 h. After the start time, the magnitude of the current was used as the control condition for constant-current accelerated corrosion. To ensure that the absorbent sponge was always in a moist state, when the solution height in the water-retaining plastic cloth was less than half of the height of the specimen, the configured NaCl solution was added until the solution height was more than 3/4 of the height of the specimen. The liquid level was kept higher than the corroded reinforcement to keep the corrosion environment stable. When the corrosion time was reached, the constant current instrument was shut down, and the fatigue test machine was stopped. When all of the specimens were loaded, the chloride-fatigue loading coupling test was performed. The corrosion conditions of each test piece are shown in Table 1.

Table 1. The Number of Samples under Different Corrosion Conditions

Sample	Loading condition (fatigue)		Corrosion condition	Sample numbers
	Stress level	Loading time(h)		
Reinforce concrete	0.3	36	5%NaCl	2
		72		2
		144		2
		216		2
	0.4	36		2
		72		2
		144		2
		216		2
	0.5	36		2
		72		2
		144		2
		216		2

2.3.3 Sample Cutting Method

The cutting method of this test is shown in Fig. 7. The specimen was cut along the marked position, and the test blocks connected with the red wire were evenly divided into 4 small blocks. The test blocks were marked from left to right as 1, 2, 3, and 4. The numbers on the sides of the test blockswere 1y1, 1z1, 2y1, 2z1, etc. (the first test block section on the left of test block 1 was marked 1z1, and the first block section on the right was marked 1y1, etc.). A 1:1 ratio of epoxy resin was applied evenly on the surface of the test block, and the test block coated with epoxy resin was cut at 15 mm to obtain a concrete slice. A cut mark was made at 5 mm around the reinforcement of the slice to obtain a

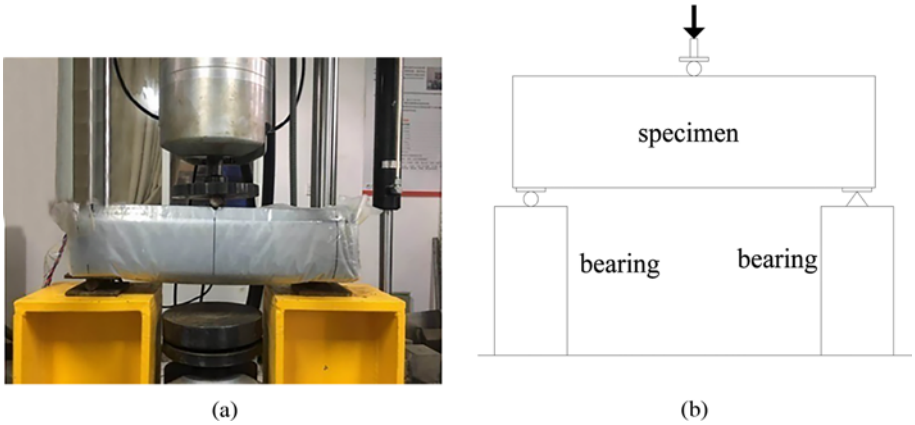

(a) (b)

Fig. 6. Specimen Loading Device: (a) Specimen Loading Device, (b) Specimen Loading Device Diagram

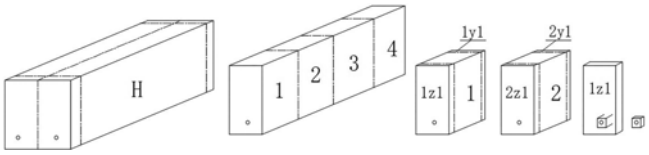

Fig. 7. Concrete Cutting Process

small square sample, and then the sample was polished to the sample requirements of scanning electron microscopy (SEM).

2.3.4 SEM Observations

Microscopic morphology observations were made using an S-4,800 field-emission scanning electron microscope produced by Hitachi, Japan (Tokyo, Japan). The surface of the sample was subjected to a gold spray treatment before the analysis. The SEM specifications were as follows: secondary electron resolution, 1.0 nm (15 kV) and 2.0 nm (1 kV); backscattered electron resolution, 3.0 nm (15 kV); acceleration voltage, 0.5 – 30 kV; cold field-emission electron source; and magnification range, 30 to 800,000 times.

2.3.5 Polycrystalline XRD Tests

The prepared powder samples were subjected to XRD (Davinci, Bruker, Germany) and analysed using JADE6.5 software. The X-ray diffractometer technical specifications are as follows: Cu target X-ray tube, voltage ≤ 50 kV, current ≤ 40 mA, nine automatic samplers, and dual optical system.

3. Quality Loss Analysis of the Corroded Reinforcement

When the corrosion time was reached, the remaining half of the specimen was disassembled, and the reinforcement connected with the blue wire was removed for derusting treatment. After the derusting was completed, the reinforcement was wiped clean, and the quality was determined (accurate to 0.001 g). Due to the influence of the stress concentration at the bearing, 40 mm test blocks at both ends of the specimen were removed during specimen cutting. Therefore, after measuring the length of the corroded reinforcement, the mass of the corroded reinforcement after cutting was proportionally converted to the corroded mass of the original length of the reinforcement, and then, the corrosion ratio of the reinforcement could be compared. The corrosion ratio of the reinforcement mass was calculated as follows:

$$L_W = \frac{W_0 - W}{W_0} \times 100\%, \quad (1)$$

where L_W is the corrosion ratio of the reinforcement mass, W_0 is the initial mass of the reinforcement before corrosion, and W is the quality of the reinforcement after derusting.

Through calculation, the corrosion ratio of the reinforcement at each corrosion time (36 h, 72 h, 144 h, and 216 h) at each stress level (0.3, 0.4, and 0.5) was obtained, as shown in Fig. 8.

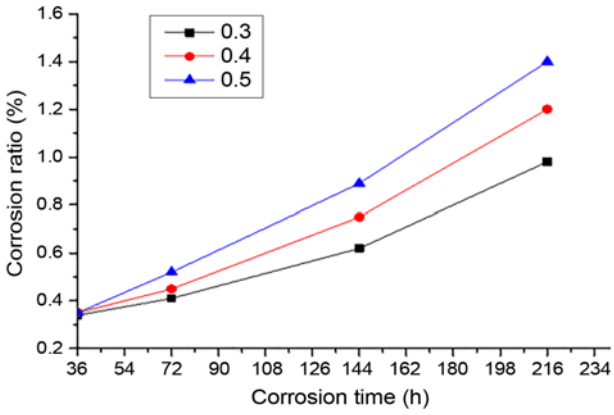

Fig. 8. Corrosion Ratio of the Reinforcement

And at each stress level (0.3, 0.4, and 0.5), there are 0.82%, 1.12%, 1.38% weight loss in 9 days, respectively.

The stress level has a significant impact on the corrosion ratio of the reinforcement. When the corrosion time is 36 h, the corrosion ratio of the reinforcement is similar at the stress levels of 0.3, 0.4 and 0.5. However, when the corrosion time is72 h, the corrosion ratio of the specimen is the highest atthe stress level of 0.5, the corrosion ratio of the specimen is the second highest at the stress level of 0.4, and the corrosion ratio of the specimen is the lowest at the stress level of 0.3, which indicates that the corrosion ratio of the reinforcement in the specimen at the stress level of 0.5 is more serious than those at the stress levels of 0.3 and 0.4. At the same stress level, the corrosion ratio of the reinforcement increases at an accelerated rate as the corrosion time increases. Different stress levels also have different effects on the corrosion ratio of the reinforcement. For the same corrosion time, the higher the stress level is, the higher the corrosion ratio of the reinforcement. Moreover, the growth rate of the corrosion ratio of the specimen at the stress level of 0.5 is significantly higher than those of the specimens at the stress levels 0.3 and 0.4, which shows that the greater the stress level is, the greater the influence on the reinforcement corrosion.

4. Fine Microanalysis of the Reinforcement/Concrete Corrosion Layer

4.1 Spatial Distribution of the Reinforcement/Concrete Interfacial Corrosion Layer

The corrosion of the reinforcement is one of the main reasons for the decline in the durability of concrete. Harmful substances enter concrete and corrode the surface of the reinforcement, leading to the deactivation of the passive film on the surface of the reinforcement and causing corrosion of the reinforcement. The volume expansion of the corrosion products produces a corrosion expansion force on the concrete around the reinforcement, resulting in concrete cracking.

According to this theory, concrete cover cracking caused by reinforcement corrosion is a process of slow development from the inside to the outside. Generally, the corrosion cracks start on

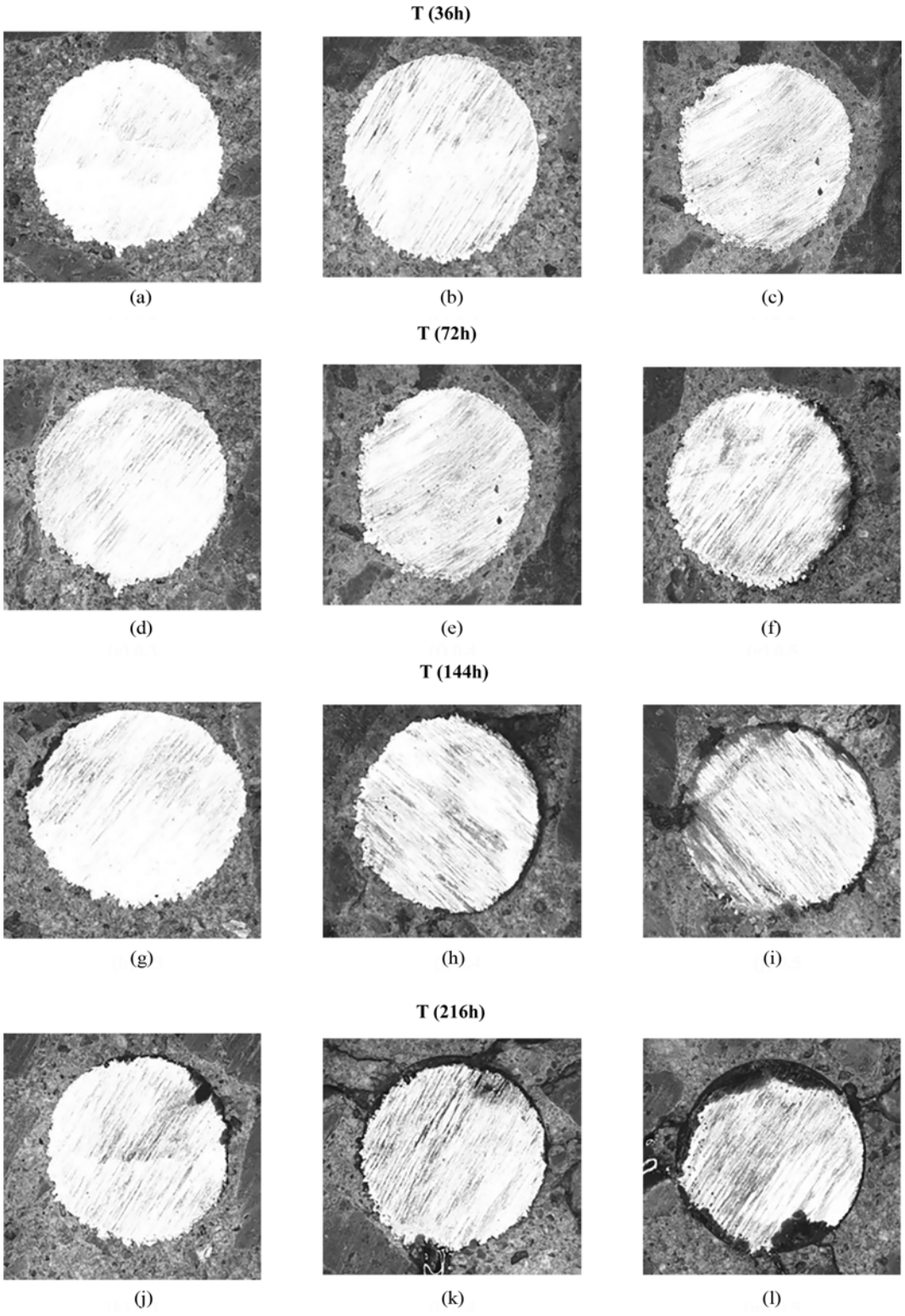

Fig. 9. Spatial Distribution of the Reinforcement/Concrete Corrosion Layer: (a) 0.3, (b) 0.4, (c) 0.5, (d) 0.3, (e) 0.4, (f) 0.5, (g) 0.3, (h) 0.4, (i) 0.5, (j) 0.3, (k) 0.4, (l) 0.5

the reinforcement surface (reinforcement corrosion products are loose, with expansive force) along with the gradually increasing development of reinforcement corrosion products, and the corrosion cracks develop from the inside to the surface of the specimen.

To study the corrosion cracking process of reinforced concrete under the action of chlorine-fatigue loading coupling and to understand the corrosion conditions of the reinforcement as well as the distribution of the corrosion layer, a test block (2y1) at the

mid-span of the specimens with different corrosion times at different stress levels was analysed using an optical microscope by mesoscale photography to obtain the corrosion conditions of the reinforcement/concrete interface.

Figures 9(j) – 9(l) show that the reinforcement corrosion mainly occurs on the side far from the concrete cover, and when the reinforcement begins to corrode, corrosion products are generated on the side far from the concrete cover. This occurs because concrete is a porous material, and the specimen is subjected to fatigue loading. The capillarity caused by the periodic opening and contraction of pores adsorbs chloride ions at the side far from the concrete cover, and thus, the chloride ions penetrate into the side far from the concrete cover. As a result, the corrosion of the reinforcement on the side far from the concrete cover is more serious than that on the other side. With increasing corrosion time, the corrosion of the reinforcement gradually becomes serious, and the corrosion layer covers half of the circumference of the reinforcement. This is different from the corrosion of reinforcement under a static load. Under static loading, cracks first appear in the tensile zone of reinforced concrete, which accelerates the penetration rate of chloride ions. Therefore, the corrosion of reinforcement is mainly concentrated on the side of the cover of the reinforcement (Zheng, 2016).

The specimen at the stress level of 0.3 do not undergo corrosion at 36 h and 72 h; the specimen at the stress level of 0.5 starts to corrode when the corrosion time is 72 h. When the corrosion time is 144 h, the corrosion product enters the crack and starts to fill the corrosion expansion crack. The fatigue stress level promotes the corrosion of the reinforcement to a certain extent. Under the same corrosion time, with increasing stress level, the corrosion of the reinforcement becomes more serious. The specimen at the stress level of 0.5 enters the third stage of reinforcement corrosion the earliest.

It can be seen from Fig. 9 hat the number and width of corrosion expansion cracks increase with increasing corrosion time, and not only do cracks appear on the side of the cover but obvious corrosion expansion cracks also occur on the side far away from the cover. These cracks are different from the corrosion expansion cracks caused by static loading (the damage caused by static loading is mainly concentrated on the side of the cover) (Zheng, 2016). The cracks in the concrete specimens have experienced an intermittent process of opening and shrinking under the action of fatigue loading, on the side far away from the cover of the reinforcement bars, the negative pressure was generated in the pore, which was connected with capillary. Under the action of capillarity, chloride ions accumulate in the pores on the upper side of the reinforcement. At the initial stage, the chloride ion concentration on the upper side of reinforcement is higher than that the other side, and the upper side of reinforcement is corroded first (Hanzic and Ilic, 2003; Ustabas, 2012) When the upper pore of reinforcement is gradually filled by corrosion products, the capillary effect is gradually weakened, but the permeability is gradually obvious. The chloride ions on the side of the concrete cover of reinforcement gradually increased, therefore, the reinforcement near the cover also began to rust.

Compared with the effect of chloride-static loading coupling, the time taken for corrosion products to enter the third stage is obviously shorter under fatigue loading. Therefore, compared with static loading, fatigue loading is more likely to cause the corrosion of the reinforcement, and this corrosion of the reinforcement is obviously more serious than that under static loading.The stress level of fatigue loading must be strictly controlled in practical engineering.

4.2 Line Scanning Energy Spectrum Analysis of the Reinforcement/Concrete Interfacial Corrosion Layer

The corrosion layer is a mixture of rust and cement hydration products. Therefore, the corrosion layer contains elements of rust and cement hydration products. Through the Fe, Ca and O elemental analyses of the corrosion layer, the position of the corrosion layer and the corrosion conditions of the reinforcement were obtained. The specimen was tested by scanning electron microscopy, and the corroded parts of the reinforcement were analysed by line scanning energy spectrum analysis (EDS), as shown in Fig. 10.

According to the mesostructural analysis of the corrosion layer of the reinforcement, the transition layer between the corroded reinforcement and concrete is filled with corrosion products. Due to the expansion of the corrosion products, the interface between the reinforcement and concrete is relatively loose, and the chemical composition changes (Shah et al., 2014). EDS was used to conduct elemental analysis of the interface area between the corroded reinforcement and concrete. The distribution order of the EDS measurement points is as follows:reinforcement matrix, reinforcement/concrete interfacial transition layer and concrete matrix at the outer edge of the corrosion layer. The relative contents of each element in the micro areas along the scan line were measured, and the Fe, Ca and O contents were measured to determine whether the reinforcement was corroded and the thickness of the corrosion layer.

As seen from Figs. 10(a) – 10(d), when the specimens are corroded for 36 h and 72 h at the stress level of 0.3, there is no overlap between Fe and Ca, indicating that no corrosion products are found. When the specimen is corroded for 144 h (Figs. 10(e) – 10(f)), Fe, Ca and O overlap in certain areas, which indicates that the reinforcement is corroded but has not penetrated the concrete matrix, and the elemental contents are low due to the cracks between the reinforcement and the concrete. When the corrosion time is 216 h (Figs. 10(g) – 10(h)), the reinforcement is corroded, and the corrosion products mainly appear on the reinforcement, indicating that corrosion occurs first on the surface of the reinforcement.

At a stress level of 0.4, when the specimen is corroded for 36 h (Figs. 10(i) – 10(j)), no corrosion products are found in the reinforcement.When the reinforcement is corroded for 72 h (Figs. 10(k) – 10(l)), the contents of Fe, Ca and O are analysed, and it is found that the surface of the reinforcement is corroded. This result occurs because the corrosion products first appear on

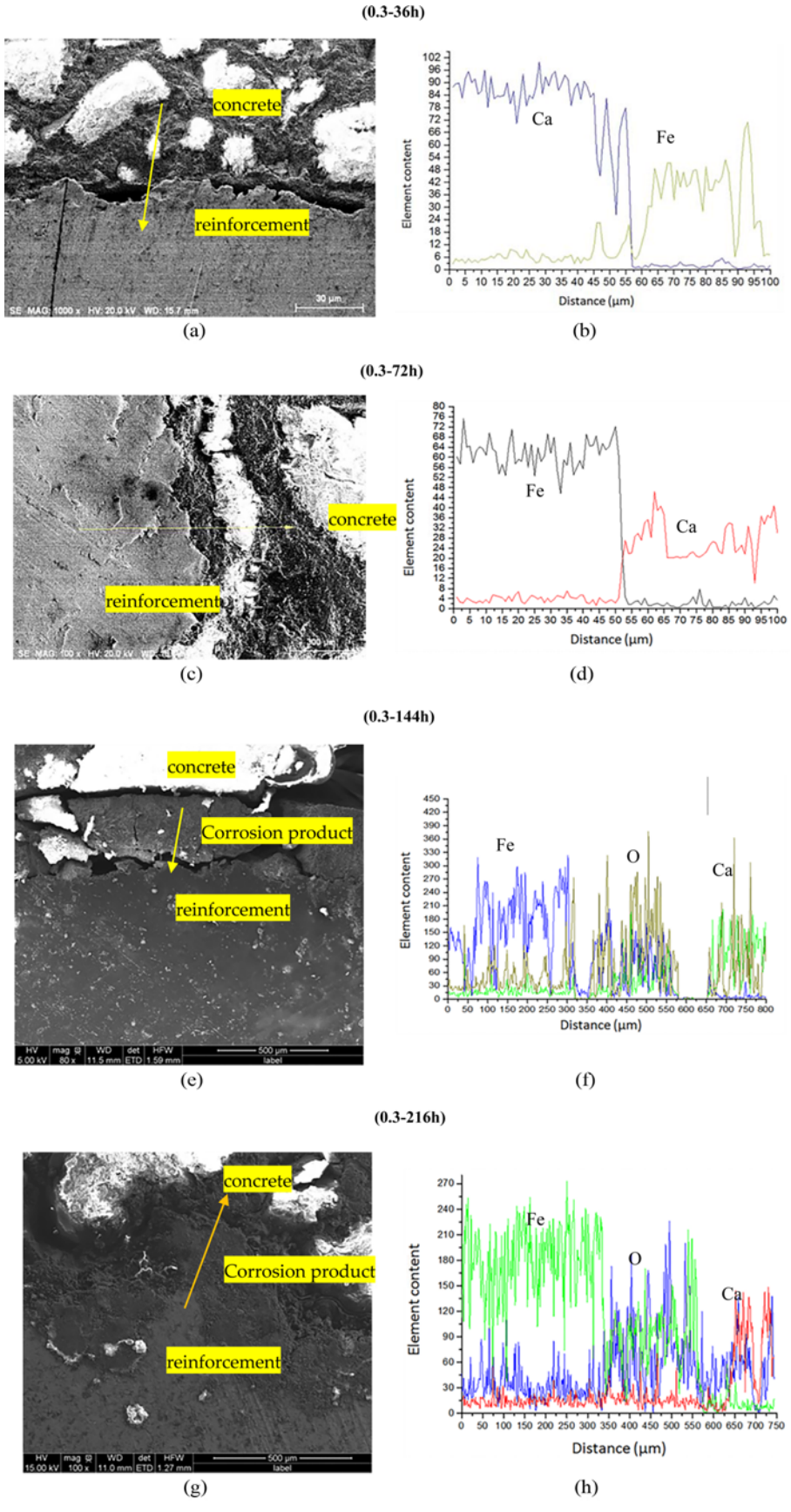

Fig. 10. EDS Analysis of the Corrosion Products: (a) 36h-SEM, (b) 36h-EDS, (c) 72h-SEM, (d) 72h-EDS, (e) 144h-SEM, (f) 144h-EDS, (g) 216h-SEM, (h) 216h-E

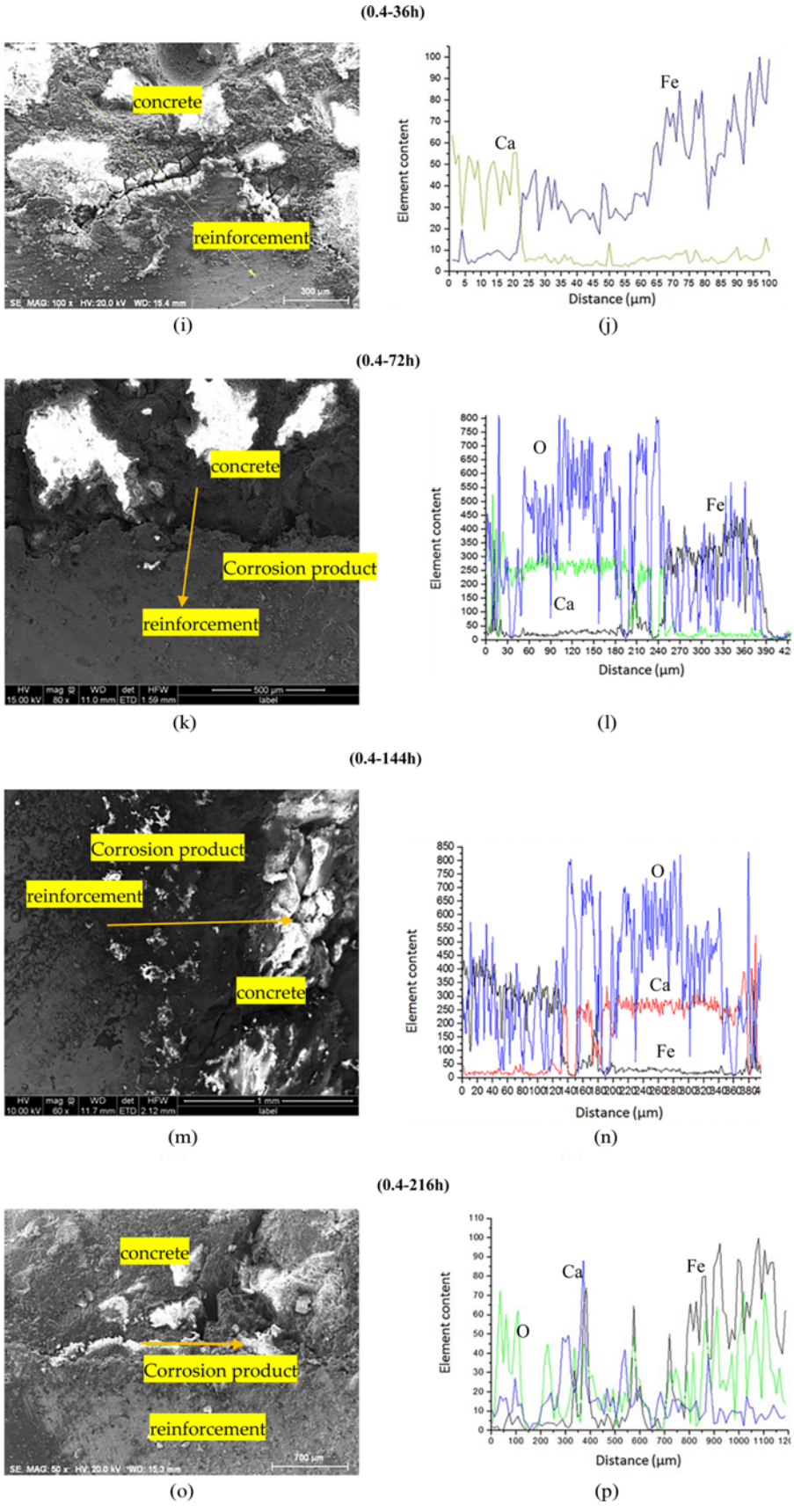

Fig. 10. (continued): (i) 36h-SEM, (j) 36h-EDS, (k) 72h-SEM, (l) 72h-EDS, (m) 144h-SEM, (n) 144h-EDS, (o) 216h-SEM, (p) 216h-EDS

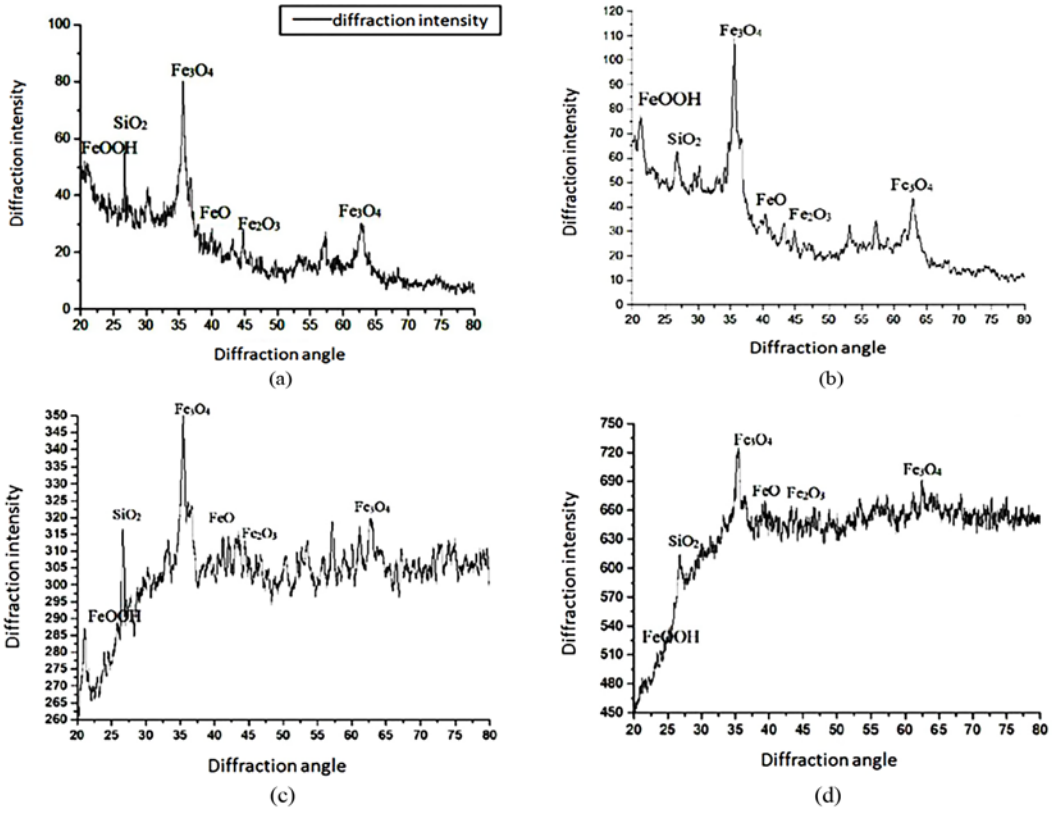

Fig. 11. X-Ray Diffraction Pattern of the Corrosion Products: (a) 0-216h, (b) 0.3-216h, (c) 0.4-216h, (d) 0.5-216h

the surface of the reinforcement at the beginning of the corrosion, and the corrosion products have not penetrated into the concrete matrix. When the reinforcement is corroded for 144 h (Figs. 10(m) – 10(n)), the thickness of the corrosion products gradually increases, and an obvious corrosion layer appears, indicating that the corrosion product on the surface of the reinforcement gradually penetrates the concrete matrix. When the reinforcement is corroded for 216 h (Figs. 10(o) – 10(p)), EDS detection is carried out on the corrosion expansion crack, and it is found that the crack contains corrosion products, indicating that the corrosion products begin to fill the crack, and the corrosion of the reinforcement enters the third stage.

EDS analysis also verifies that the fatigue stress level promotes the corrosion of the reinforcement to a certain extent. Under the same corrosion time, the corrosion of the reinforcement increases with an increase in the stress level.

4.3 XRD Analysis of the Corrosion Products

The corrosion products on the surface of the corroded reinforcement were analysed. The reinforcement bars connected with the blue wire were removed from the specimen, and the corrosion products on the surface of the reinforcement were scraped with a blade. The corrosion products with a corrosion time of 216 h at each stress level (0.3, 0.4, and 0.5) and no loading (0) were selected for X-ray diffraction analysis. The test results are shown in Fig. 11. The types of corrosion products have been obtained by XRD of Fig. 11 and Table 2. The corrosion products of natural corrosion was consistent with artificial corrosion (Vera et al., 2009; Gan et al., 2011; Du et al., 2020).

Table 2. Proportion of the Corrosion Product Content

Name	0.3-216h	0.4-216h	0.5-216h	Noloading
Fe_3O_4	53.71%	71.69%	53.53%	59.01%
FeOOH	31.37%	1.80%	26.52%	27.12%
Fe_2O_3	12.59%	24.33%	11.74%	12.54%
FeO	2.33%	2.18%	8.21%	1.43%

The corrosion products of the reinforcement are mainly Fe_3O_4, SiO_2, FeOOH, Fe_2O_3, and FeO, among which Fe_3O_4 has the highest diffraction intensity and content compared with the other concentrated corrosion products, and the peak value of Fe_3O_4 is obviously increasing. At a stress level of 0.5, the peak diffraction intensity of each corrosion product in the specimen is more obvious than those at the stress levels of 0.3 and 0.4, indicating that at a corrosion time of 216 h, the greater the stress level is, the more serious the reinforcement corrosion. The proportions of components in the corrosion products at the corrosion time of 216 h at each stress level were measured, as shown in Table 2.

Based on Fig. 11 and Table 2, at a corrosion time of 216 h, the corrosion products of the reinforcement at various stress levels

and no loading are consistent with each other, but the material composition ratios are not the same. In accelerated corrosion tests of reinforced concrete, chloride ions enter the concrete interior through the pores in the concrete and reach the surface of the reinforcement. The chloride ions depolarise the reinforcement, producing Fe^{2+} on the surface. Fe^{2+} forms $FeCl_2$ with Cl^- on the surface of the reinforcement, and $FeCl_2$ is a soluble substance. $FeCl_2$, as an intermediate, is transported along the surface of the reinforcement at the reinforcement/concrete interface, and thus, the chloride content does not decrease in solution. When $FeCl_2$ encounters OH^-, $Fe(OH)_2$ immediately precipitates and forms $Fe(OH)_3$ under oxygen-enriched conditions, and $Fe(OH)_3$ is dehydrated to form loose and porous Fe_2O_3, among which FeOOH is formed when the dehydration is not complete. Under anoxic conditions, incompletely oxidised $Fe(OH)_2$ forms Fe_3O_4. Therefore, the phase content of reinforcement corrosion products mainly depends on the oxygen content. The proportion of Fe_3O_4 is the highest in the corrosion products at various stress levels, the proportions of Fe_2O_3 and FeOOH are in the middle, and the proportion of FeO is the lowest, indicating that the corrosion products of the reinforcement mainly occur in a hypoxic environment. As seen from Figs. 11(c) – 11(d), with increasing stress level and corrosion time, the content of Fe_2O_3 increases significantly, which also indicates that cracking increases the oxygen supply of the corrosion environment and accelerates the process of corrosion, and this is consistent with the actual conditions.

5. Structural Model of the Corrosion Cracking of Concrete under Chloride-Fatigue Loading Coupling

For the corrosion cracking process of concrete covers caused by reinforcement corrosion, the most widely accepted theory at present is the “three-stage theory” of reinforcement corrosion cracking (Liu and Weyers, 1998; Pantazopoulou and Papoulia, 2001; Wang and Liu, 2004; Wong et al., 2010): ① the reinforcement begins to corrode, and the resulting corrosion products fill the pores of the reinforcement/concrete interface, as shown in Fig. 12(b); ② when the corrosion products fill the original cracks and pores, corrosion products continue to form with a certain expansion force, causing cracks in the reinforcement/concrete interface, as shown in Fig. 11(c); and ③ cracks appear in the cover, the cracks develop, and corrosion products fill the cracks, as shown in Fig. 12(d).

Previously, scholars believed that the three stages of the corrosion cracking process occur in sequence, but this paper found that the first stage and the second stage occurred simultaneously. In the process of filling the interface gap with corrosion products after the corrosion of the reinforcement, cracks have been produced; when the corrosion on the reinforcement surface reaches a certain amount, it gradually penetrates into the concrete matrix, while corrosion on the side of the reinforcement matrix continues to occur. When the corrosion products fill the pores, corrosion expansion cracks will be generated.

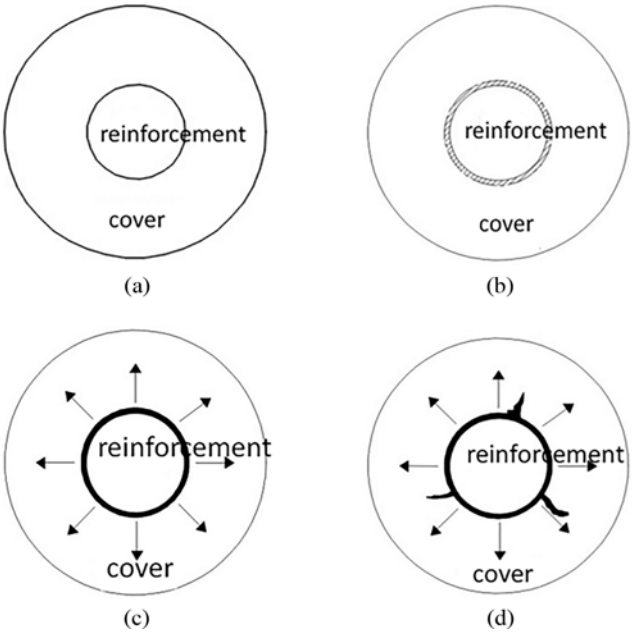

Fig. 12. Three-Stage Reinforcement Corrosion Structural Model: (a) Initial, (b) Reinforcement Begins to Corrode, (c) Corrosion Expansion of Reinforcement/Concrete Interface, (d) Cracks Appear in the Cover

Due to fatigue loading on the specimen, the capillary action caused by the periodic opening and contraction of pores adsorbs chloride ions to the side away from the cover so that the side away from the cover begins to corrode, as shown in Fig. 12(a). With the increase in the corrosion time, the corrosion products gradually increase, and the corrosion of the reinforcement gradually intensifies. The corrosion on the side of the reinforcement away from the cover deepens, and the corrosion products gradually spread to the interior of the reinforcement. However, after spreading to a certain extent, the corrosion products began to penetrate into the concrete matrix, and at the same time, the corrosion products began to form on the side of the cover of the reinforcement, as shown in Fig. 13(b). Under the action of fatigue loading, the corrosion products of the reinforcement gradually changed from fluffy and porous to dense and multilayer and began to produce a certain corrosion expansion force. Moreover, under the fatigue loading, the capillary action caused by the periodic opening and contraction of the pores results in corrosion expansion cracks, which is different from that under the static loading (the corrosion expansion cracks under static loading are concentrated on the side of the cover of the reinforcement, and the cracks of corrosion expansion under fatigue loading are separated by 120°), as shown in Fig. 13(c). As the corrosion of reinforcement is gradually intensified, the corrosion products fill into the corrosion expansion crack, and the corrosion range of the reinforcement on the side away from the cover gradually covers half of the circumference of the reinforcement, as shown in Fig. 13(d).

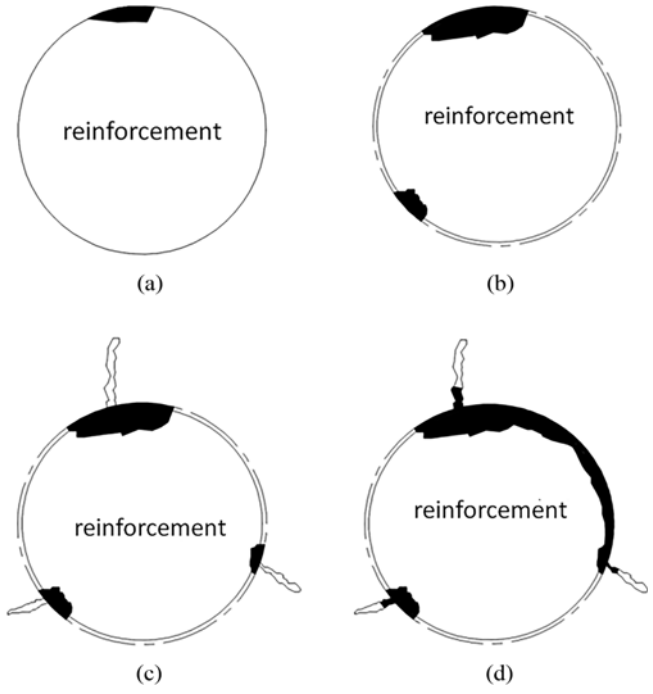

Fig. 13. Reinforcement Corrosion Structural Model: (a) Corrosion of the Side Away from the Cover, (b) Corrosion on Both Sides of Reinforcement, (c) Corrosion Expansion Cracks Separated by 120°, (d) Corrosion Products Fill into Crack

6. Conclusions

1. Through the analysis of the quality loss of the reinforcement, the corrosion of steel bars at different corrosion times at different stress levels is analysed. Under the same stress, the corrosion of the reinforcement increases with increasing corrosion time. For the same corrosion time, the corrosion of the reinforcement increases with an increase in the stress level.
2. Through the analysis of the spatial distribution of the Reinforcement/concrete interfacial corrosion layer, The corrosion of the reinforcement occurs mainly on the side far from the concrete cover because concrete is a porous material. Due to fatigue loading on the specimen, the capillary action caused by the periodic opening and contraction of the pores causes chloride ions to be adsorbed on the side far from the cover, resulting in more serious corrosion of the reinforcement on the side far from the cover than on the side of the cover.
3. The corrosion cracking process of reinforced concrete under chloride-fatigue loading coupling is divided into the following four stages: stage 1, the surface of the reinforcement begins to corrode, mainly on the side far from the cover; stage 2, the corrosion products on the surface of the reinforcement gradually spread to the interior of the reinforcement, corrosion occurs on the side of the cover of the reinforcement, and corrosion products gradually penetrate into the concrete; stage 3, the corrosion products that infiltrate into the concrete have a certain corrosion expansion force, creating expansion cracks in the concrete; and stage 4, the generated corrosion products gradually fill the corrosion expansion cracks.

Acknowledgments

The authors wish to acknowledge the financial support of the National Natural Science Foundation of China (Grant No. 51778577, 51778302, 51778578), the Natural Science Foundation of Zhejiang (Grant No. LY17E080017) and the Natural Science Foundation of Ningbo(Grant No. 2019A610401).

ORCID

Jiansheng Shen https://orcid.org/0000-0003-2975-487X
Junzhe Liu https://orcid.org/0000-0001-7246-1621
Yidong Xu https://orcid.org/0000-0003-3756-032X
Wei Chen https://orcid.org/0000-0002-5387-6554
Dayong Zhu https://orcid.org/0000-0001-8285-2634

References

Adelaide L, Richard B, Ragueneau F, Cremona C (2012) A simplified numerical approach of global behaviour of RC beams degraded by corrosion. *European Journal of Environmental and Civil Engineering* 16(3-4):414-439, DOI: 10.1080/19648189.2012.667990

Ahn W, Reddy DV (2001) Galvanostatic testing for the durability of marine concrete under fatigue loading. *Cement and Concrete Research* 31(3):343349, DOI: 10.1016/S0008-8846(00)00506-8

Asami K, Kikuchi M (2003) In-depth distribution of rusts on a plain carbon steel and weathering steels exposed to coastal – industrial atmosphere for 17 years. *Corrosion Science* 45(11):2671-2688, DOI: 10.1016/S0010-938X(03)00070-2

Azad AK, Ahmad S, Al-Gohi BHA (2010) Flexural strength of corroded reinforced concrete beams. *Magazine of Concrete Research* 62(6): 405-414, DOI: 10.1680/macr.2010.62.6.405

Bastidas-Arteaga E (2018) Reliability of reinforced concrete structures subjected to corrosion-fatigue and climate change. *International Journal of Concrete Structures and Materials* 12(1):10, DOI: 10.1186/s40069-018-0235-x

Coca FJO, Tello MUL, Gaona-Tiburcio C, Romero JA, Martínez-Villafañe A, Maldonado BE, Almeraya-Calderon F (2011) Corrosion fatigue of road bridges: A review. *International Journal of Electrochemical Science* 6:3438-3451

Dekoster M, Buyle-Bodin F, Maurel O, Delmas Y (2003) Modelling of the flexural behaviour of RC beams subjected to localised and uniform corrosion. *Engineering Structures* 25(10):1333-1341, DOI: 10.1016/S0141-0296(03)00108-1

Dong JF, Zhao Y, Wang K, Jin WL (2017) Crack propagation and flexural behaviour of RC beams under simultaneous sustained loading and steel corrosion. *Construction and Building Materials* 151:208-219, DOI: 10.1016/j.conbuildmat.2017.05.193

Du FY, Jin ZQ, She W, Xiong CS, Fan JF (2020) Chloride ions migration and induced reinforcement corrosion in concrete with cracks: A comparative study of current acceleration and natural marine exposure. *Construction and Building Materials* 263:120099, DOI: 10.1016/j.conbuildmat.2020.120099

Duffo GS, Morris W, Raspini I, Saragovi C (2004) A study of steel rebars embedded in concrete during 65 years. *Corrosion Science* 46

(9):2143-2157, DOI: 10.1016/j.corsci.2004.01.006
Fang C, Yang S, Zhang Z (2013) Bending characteristics of corroded reinforced concrete beam under repeated loading. *Structural Engineering and Mechanics* 47(6):773-790, DOI: 10.12989/sem.2013.47.6.773
Gan WZ, Jin WL, Gao MZ (2011) Applicability study on accelerated corrosion methods of steel bars in concrete structure. *Jianzhu Jiegou Xuebao/Journal of Building Structures* 32(2):41-47 (in Chinese)
GB/T 50082-2009 (2009) Standard for methods of long-term performance and durability of ordinary concrete. GB/T 50082-2009, China Architectural Industry Press, Beijing, China, 119-120
Hanzic L, Ilic R (2003) Relationship between liquid sorptivity and capillarity in concrete. *Cement and Concrete Research* 33(9):1385-1388, DOI: 10.1016/S0008-8846(03)00070-X
Hartt WH (2012) Service life projection for chloride-exposed concrete reinforced with black and corrosion-resistant bars. *Corrosion* 68(8):754-761, DOI: 10.5006/0489
Higgins L, Forth JP, Neville A, Jones R, Hodgson T (2013) Behaviour of cracked reinforced concrete beams under repeated and sustained load types. *Engineering Structures* 56:457-465, DOI: 10.1016/j.engstruct.2013.05.034
Jin WL, Zhao YX (2014) Durability of concrete structure. Science Press, Beijing, China, 40-41
Liu QF, Feng GL, Xia J, Yang J, Li LY (2018) Ionic transport features in concrete composites containing various shaped aggregates: A numerical study. *Composite Structures* 183:371-380, DOI: 10.1016/j.compstruct.2017.03.088
Liu QF, Hu Z, Lu XY, Yang J, Azim I, Sun W (2020) Prediction of chloride distribution for offshore concrete based on statistical analysis. *Materials* 13(1):174, DOI: 10.3390/ma13010174
Liu YP, Weyers RE (1998) Modeling the time-to-corrosion cracking in chloride contaminated reinforced concrete structures. *ACI Materials Journal* 95(6):675-681
Lu YY, Tang W, Li S, Tang MY (2018) Effects of simultaneous fatigue loading and corrosion on the behavior of reinforced beams. *Construction and Building Materials* 181:85-93, DOI: 10.1016/j.conbuildmat.2018.06.028
Lu C, Yuan S, Cheng P, Liu RG (2016) Mechanical properties of corroded steel bars in pre-cracked concrete suffering from chloride attack. *Construction and Building Materials* 123:649-660, DOI: 10.1016/j.conbuildmat.2016.07.032
Malumbela G, Moyo P, Alexander M (2009) Behaviour of RC beams corroded under sustained service loads. *Construction and Building Materials* 23(11):3346-3351, DOI: 10.1016/j.conbuildmat.2009.06.005
Mao JH, Xu FY, Jin WL, Zhang J, Wu XX, Chen CS (2018) Research on the fatigue flexural performance of RC beams attacked by salt spray. *China Ocean Engineering* 32(2):179-188, DOI: 10.1007/s13344-018-0019-8 (in Chinese)
Marcotte TD, Hansson CM (2007) Corrosion products that form on steel within cement paste. *Materials and Structures* 40(3):325-340, DOI: 10.1617/s11527-006-9170-4
Nie J, Wang Y, Cai CS (2011) Experimental research on fatigue behavior of RC beams strengthened with steel plate-concrete composite technique. *Journal of Structural Engineering* 137(7):772-781, DOI: 10.1061/(ASCE)ST.1943-541X.0000336
Oh BH, Kim SH (2007) Advanced crack width analysis of reinforced concrete beams under repeated loads. *Journal of Structural Engineering* 133(3):411-420, DOI: 10.1061/(ASCE)0733-9445(2007)133:3(411)
Oyado M, Hasegawa M, Sato T (2003) Characteristics of fatigue and evaluation of RC beam damaged by accelerated corrosion. *Quarterly Report of RTRI* 44(2):72-77, DOI: 10.2219/rtriqr.44.72
Pantazopoulou SJ, Papoulia K D (2001) Modeling cover cracking due to reinforcement corrosion in R.C. structures. *Journal of Engineering Mechanics* 127(4):342-346, DOI: 10.1061/(ASCE)0733-9399(2001)127:4(342)
Pimentel M, Brühwiler E, Figueiras J (2008) Fatigue life of short-span reinforced concrete railway bridges. *Structural Concrete* 9(4):215-222, DOI: 10.1680/stco.2008.9.4.215
Ray S, Kishen JMC (2014) Analysis of fatigue crack growth in reinforced concrete beams. *Materials and Structures* 47(1-2):183-198, DOI: 10.1617/s11527-013-0054-0
Ren Y, Huang Q, Liu QY, Sun JZ, Liu XL (2015) Chloride ion diffusion of structural concrete under the coupled effect of bending fatigue load and chloride. *Materials Research Innovations* 19:181-184, DOI: 10.1179/1432891715Z.0000000001400
Rodriguez J, Ortega LM, Casal J (1997) Load carrying capacity of concrete structures with corroded reinforcement. *Construction and Building Materials* 11(4):239-248, DOI: 10.1016/S0950-0618(97)00043-3
Shah SG, Ray S, Kishen JMC (2014) Fatigue crack propagation at concrete–concrete bi-material interfaces. *International Journal of Fatigue* 63:118-126, DOI: 10.1016/j.ijfatigue.2014.01.015
Sheng J, Yin SP, Wang F, Yang Y (2017) Experimental study on the fatigue behaviour of RC beams strengthened with TRC after sustained load corrosion. *Construction and Building Materials* 131:713-720, DOI: 10.1016/j.conbuildmat.2016.11.030
Sousa C, Calçada R, Neves AS (2014) Numerical evaluation of the non-linear behaviour of cracked RC members under variable-amplitude cyclic loading. *Materials and Structures* 48:2815-2838, DOI: 10.1617/s11527-014-0356-x
Sun J, Huang Q, Ren Y (2015) Performance deterioration of corroded RC beams and reinforcing bars under repeated loading. *Construction and Building Materials* 96:404-415, DOI: 10.1016/j.conbuildmat.2015.08.066
Torres-Acosta AA, Navarro-Gutierrez S, Terán-Guillén J (2007) Residual flexure capacity of corroded reinforced concrete beams. *Engineering Structures* 29(6):1145-1152, DOI: 10.1016/j.engstruct.2006.07.018
Ustabas I (2012) The effect of capillarity on chloride transport and the prediction of the accumulation region of chloride in concretes with reinforcement corrosion. *Construction and Building Materials* 28(1):640-647, DOI: 10.1016/j.conbuildmat.2011.10.043
Vera R, Villarroel M, Carvajal AM, Vera E, Ortiz C (2009) Corrosion products of reinforcement in concrete in marine and industrial environments. *Materials Chemistry and Physics* 114(1):467-474, DOI: 10.1016/j.matchemphys.2008.09.063
Vu KAT, Stewart MG (2000) Structural reliability of concrete bridges including improvedchloride-induced corrosion models. *Structural Safety* 22(4):313-33, DOI: 10.1016/S0167-4730(00)00018-7
Vu HH, Vu NA, François R (2014) Effect of corrosion of tensile rebars and stirrups on the flexural stiffness of reinforced concrete members. *European Journal of Environmental and Civil Engineering* 18(3):358-376, DOI: 10.1080/19648189.2014.881759
Wang XH, Bastidas-Arteaga E, Gao Y (2018a) Probabilistic analysis of chloride penetration in reinforced concrete subjected to pre-exposure static and fatigue loading and wetting-drying cycles. *Engineering Failure Analysis* 84:205-219, DOI: 10.1016/j.engfailanal.2017.11.008
Wang JH, Cai G, Wu Q (2018b) Basic mechanical behaviours and deterioration mechanism of RC beams under chloride-sulphate environment. *Construction and Building Materials* 160:450-461, DOI: 10.1016/j.conbuildmat.2017.11.092
Wang XH, Liu XL (2004) Modelling effects of corrosion on cover

cracking and bond in reinforced concrete. *Magazine of Concrete Research* 56(4):191-199, DOI: 10.1680/macr.56.4.191.36306

Wang L, Ma Y, Ding W, Zhang J, Liu Y (2015) Comparative study of flexural behavior of corroded beams with different types of steel bars. *Journal of Performance of Constructed Facilities* 29(6):04014163, DOI: 10.1061/(ASCE)CF.1943-5509.0000661

Williamson SJ, Clark LA (2000) Pressure required to cause cover cracking of concrete due to reinforcement corrosion. *Magazine of Concrete Research* 52(6):455-467, DOI: 10.1680/macr.2000.52.6.455

Wong HS, Zhao YX, Karimi AR, Buenfeld NR, Jin WL (2010) On the penetration of corrosion products from reinforcing steel into concrete due to chloride-induced corrosion. *Corrosion Science* 52(7):2469-2480, DOI: 10.1016/j.corsci.2010.03.025

Wu JQ, Diao B, Xu JC, Zhao RX, Zhang WM (2020) Effects of the reinforcement ratio and chloride corrosion on the fatigue behavior of RC beams. *International Journal of Fatigue* 131(2):1-12, DOI: 10.1016/j.ijfatigue.2019.105299

Wu J, Faye PPN, Zhang W, Diao B (2018) Chloride diffusivity and service life prediction of RC columns with sustained load under chloride environment. *Construction and Building Materials* 158:97-107, DOI: 10.1016/j.conbuildmat.2017.10.018

Xia J, Jin WL, Li LY (2011) Shear performance of reinforced concrete beams with corroded stirrups in chloride environment. *Corrosion Science* 53(5):1794-1805, DOI: 10.1016/j.corsci.2011.01.058

Xu YD, Shen JS, Zheng YY, Mao JH, Wu P (2018) Corrosion characteristics of reinforced concrete under the coupled effects of chloride ingress and static loading: Laboratory tests and finite element analysis. *Materials Science* 24(2):212-217, DOI: 10.5755/j01.ms.24.2.17963

Yi WJ, Kunnath SK, Sun XD, Tang FJ (2010) Fatigue behavior of reinforced concrete beams with corroded steel reinforcement. *ACI Materials Journal* 107(5):526-533, DOI: 10.1016/j.conbuildmat.2015.12.119, DOI: 10.1061/(ASCE)CC.1943-5614.0000144

Yu L, François R, Dang VH, Hostis VL, Gagné R (2015) Structural performance of RC beams damaged by natural corrosion under sustained loading in a chloride environment. *Engineering Structures* 96:30-40, DOI: 10.1016/j.engstruct.2015.04.001

Zhang K, Zhang J, Jin WL, Mao JH, Long JX (2020) Stiffness degradation for fatigue of reinforced concrete beams after electrochemical rehabilitation. *Construction and Building Materials* 260:1-12, DOI: 10.1016/j.conbuildmat.2020.120455

Zheng YY (2016) Multi-scale analysis of corrosion behavior of steel bar in reinforced concrete under coupled interaction between environment factors and loading. MSc Thesis, Chongqing Jiaotong University, Chongqing, China (in Chinese)

Zhu W, François R (2014) Corrosion of the reinforcement and its influence on the residual structural performance of a 26-year-old corroded RC beam. *Construction and Building Materials* 51:461-472, DOI: 10.1016/j.conbuildmat.2013.11.015